

Casimir Force in Anisotropic Materials with AC Kerr Effect

Junlong Zhang¹, Zhixiang Huang^{1, *}, and Xianliang Wu^{1, 2}

Abstract—The Casimir force between an ellipsoid and a plate can be tuned by using the combination of anisotropic materials and nonlinear materials exhibiting the AC Kerr effect. The force was obtained numerically by using the FDTD method, based on the Maxwell's stress tensor. The results indicate that the force can be significantly varied by changing the intensity and location of the laser, as well as the properties of material. The sensitive changing between ellipsoid and plate structure with different materials' properties provides new possibilities of integrating optical devices into nano-electro-mechanical systems (NEMS).

1. INTRODUCTION

In 1948 Casimir [1] found that a pair of neutral, perfectly conducting parallel plates located in vacuum attracted each other. Then, the existence of the Casimir force had been considered the focus of attention over decades, and various numerical calculations have been developed [2]. Two main calculation methods are the surface mode summation method [3], and the stress tensor method [4]. Then, efforts have been made to study the Casimir force for various geometries and materials [5–7]. However, in most cases the force was found to be attractive [8].

With the advances of fabrication techniques in the micro-electro-mechanical systems (MEMS) and nano-electro-mechanical systems (NEMS), the device size had become smaller and smaller. Scaling issues become the hot topic in recent year, especially in the nano-optoelectronic system. The diminishing scaling will inevitably bring upon the issue of Casimir attractive interaction between dielectric and metallic surfaces in close spacing. For example, the attractive force can cause the stiction problem [9–11]. The problem may be resolved if the Casimir force is repulsive [8, 12]. Therefore, repulsive Casimir force received unprecedented attention in practical systems [13, 14].

Anisotropy is a material's directional dependence of a physical property, as opposed to isotropy. In electromagnetism it can be defined as a difference, when measured along different axes, in a material's electromagnetic properties like electric permittivity ε , magnetic permeability μ . Here we consider the electric permittivity tensor form of second order with

$$\varepsilon = \begin{pmatrix} a & u & v \\ u & b & w \\ v & w & c \end{pmatrix} \quad (1)$$

Set $u = v = w = 0$ to simplify the tensor. When $a = b = c \neq 0$, the material is isotropy; when $a = b \neq c \neq 0$, the material is uniaxial anisotropy; when $a \neq b \neq c \neq 0$, the material is biaxial anisotropy.

AC Kerr effect is an optical phenomenon that a laser beam in a medium can itself provide the modulating electric field, without the need for an external field to be applied [15]. It is a nonlinear optical effect due to the third order polarization of the laser field. It is possible to use the effect

Received 21 July 2014, Accepted 4 September 2014, Scheduled 10 September 2014

* Corresponding author: Zhixiang Huang (zxhuang@ahu.edu.cn).

¹ Key Lab of Intelligent Computing & Signal Processing, Anhui University, Ministry of Education, Hefei 230039, China. ² Department of Physics and Electronic Engineering, Hefei Normal University, Hefei 230061, China.

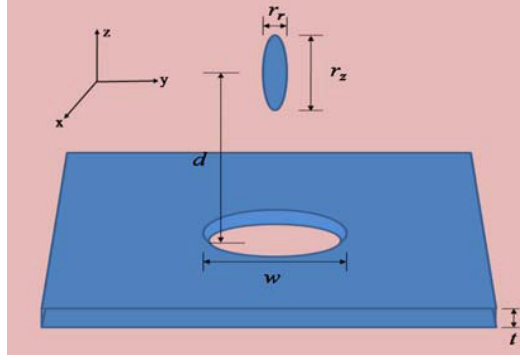


Figure 1. Geometry for achieving Casimir force: A metal ellipsoid above a thin metal plate with a hole. d is the center-center separation, w the plate hole width, t the thickness of the plate, r_r the minor diameter of the ellipsoid, and r_z the major diameter of the ellipsoid. The shaded part indicates different material.

to control the Casimir force [16] between the ellipsoid and the plate with a hole, as shown in Fig. 1, corresponding to a constitutive relation: $\mathbf{D} = (\varepsilon_0 + \chi^{(3)} \cdot |\mathbf{E}|^2) \mathbf{E}$, $\chi^{(3)}$ is a susceptibility that characterized the Kerr nonlinearities. However, the number usually reported for the strength of the Kerr nonlinearity is the Kerr coefficient n_2 , defined by the effective change in refractive index Δn for a plane wave with time-average intensity I traveling through a homogeneous Kerr material: $\Delta n = n_2 I$. The relationship between n_2 and $\chi^{(3)}$ is $n_2 = \frac{3\chi^{(3)}}{4n^2}$, unit $\mu\text{m}^2/\text{w}$, where n is the linear refractive index $n = \sqrt{\varepsilon}$. Therefore, we can use the Kerr material instead of laser field.

2. NUMERICAL IMPLEMENTATION

The key point of the approach is to compute the force via a series of independent FDTD [17] calculations in which sources are separately placed at each point on S , calculate the entire frequency spectrum in a single simulation for each source, and then integrate the electromagnetic response in time domain against a predetermined function $g(-t)$ [18, 19].

2.1. Maxwell's Stress Tensor Formulation

Classically, the force on an object due to the electromagnetic field can be obtained by integrating the Maxwell's stress tensor over frequency and around a surface enclosing the object, which is

$$F_i = \int_0^\infty d\omega \oint_S \sum_j \langle M_{ij}(r, \omega) \rangle dS_j \quad (2)$$

where r denotes spatial position and ω frequency. When integrated over imaginary frequencies $\omega = i\xi$, the expression becomes

$$F_i = \text{Im} \int_0^\infty \frac{d\omega}{d\xi} d\xi \oint_S \sum_j \langle M_{ij}(r, \omega) \rangle dS_j \quad (3)$$

where the stress tensor is expressed in terms of correlation functions of the field operators $\langle E_i(r, \omega) E_j(r', \omega) \rangle$ and $\langle H_i(r, \omega) H_j(r', \omega) \rangle$ as

$$\begin{aligned} \langle M_{ij}(r, \omega) \rangle = & \mu(r, \omega) \left[\langle H_i(r, \omega) H_j(r, \omega) \rangle - \frac{1}{2} \delta_{ij} \sum_k \langle H_k^2(r, \omega) \rangle \right] \\ & + \varepsilon(r, \omega) \left[\langle E_i(r, \omega) E_j(r, \omega) \rangle - \frac{1}{2} \delta_{ij} \sum_k \langle E_k^2(r, \omega) \rangle \right] \end{aligned} \quad (4)$$

The average of fluctuating electric and magnetic fields in the ground state is given via the fluctuation-dissipation theorem in terms of the photon Green's function [20]:

$$\langle E_i(r, \omega) E_j(r', \omega) \rangle = \frac{\hbar}{\pi} \omega^2 \text{Im} G_{ij}^E(\omega; r, r') \quad (5)$$

$$\langle H_i(r, \omega) H_j(r', \omega) \rangle = -\frac{\hbar}{\pi} (\nabla \times)_{il} (\nabla' \times)_{jm} \text{Im} G_{lm}^E(\omega; r, r') \quad (6)$$

where the photon Green's function G_{ij}^E satisfies the equation

$$\left[\nabla \times \nabla \times \frac{-w^2}{\mu(r, \omega)} \varepsilon(r, \omega) \right] G_j^E(\omega; r, r') = \delta(r - r') \hat{e}_j \quad (7)$$

2.2. Harmonic Expansion in Cylindrical Coordinates

The most practical harmonic expansion basis which consists of functions of form is $f_n(x)e^{im\phi}$. When in a cylindrical symmetry, as shown in our geometry, we can employ the cylindrical surface S and complex exponential basis $e^{im\phi}$ in the ϕ direction in a cylindrical coordinates. Thus, the resulting fields are separable with ϕ , and the equations only contain the (r, z) coordinates. Then the calculation reduces to a 2D problem for each m . Once the fields are determined in (r, z) coordinates, the force contribution for each m is [19]

$$F_{i;m} = \int_0^{2\pi} d\phi \int_S ds_j(\mathbf{x}) r(\mathbf{x}) e^{-im\phi} \int_0^{2\pi} d\phi' \times \int_S ds(\mathbf{x}') r(\mathbf{x}') e^{im\phi'} \delta_S(\mathbf{x} - \mathbf{x}') \Gamma_{ij;m}(t; \mathbf{x}, \mathbf{x}') \quad (8)$$

where \mathbf{x} ranges over the full three dimensional coordinates. For simplicity, assume that S consists entirely of $z = \text{const}$ and $r = \text{const}$ surfaces. In these cases, the surface δ function δ_S is given by [19]

$$\begin{aligned} \delta_S(\mathbf{x} - \mathbf{x}') &= \frac{1}{2\pi r(\mathbf{x})} \delta(\phi - \phi') \delta(r - r'), \quad z = \text{const} \\ \delta_S(\mathbf{x} - \mathbf{x}') &= \frac{1}{2\pi r(\mathbf{x})} \delta(\phi - \phi') \delta(z - z'), \quad r = \text{const} \end{aligned} \quad (9)$$

$\Gamma_{ij;m}$ are functions of the electromagnetic fields on the surface S . $r(\mathbf{x})$ is the Jacobian factor and ds the Cartesian line element. Where $ds_j(\mathbf{x}) = ds(\mathbf{x}) n_j(\mathbf{x})$, $n(\mathbf{x})$ is the unit normal vector to S at \mathbf{x} .

Accordingly, the current source of three-dimensional coordinates is $f_n(\mathbf{x}) e^{im\phi} = \delta(\mathbf{x} - \mathbf{x}') e^{im\phi}$, so the field must have a ϕ dependence of the form $e^{im\phi}$ as $\Gamma_{ij;nm}(r, z, \phi, t) = \Gamma_{ij;nm}(r, z, t) e^{im\phi}$.

2.3. Geometry-Independent Function $g(-t)$

In [19], the authors introduced a geometry-independent function $g(-t)$, which resulted from the Fourier transform of a certain function of frequency, termed $g(\xi)$ and is given by

$$g(\xi) = -i\xi \left(1 + \frac{i\sigma}{\xi} \right) \frac{1 + i\sigma/2\xi}{\sqrt{1 + i\sigma/\xi}} \Theta(\xi) \quad (10)$$

here, the $\Theta(\xi)$ is the unit-step function for later convenience.

Once $g(-t)$ is known, it can be integrated against the fields in time to obtain the correct Casimir force. As discussed in [18], in the time domain of the cylindrical system the Fourier transform can be performed analytically, and the result is

$$\text{Img}(-t) = \frac{1}{2\pi} \left(\frac{2}{t^3} + \frac{3\sigma}{2t^2} + \frac{\sigma^2}{2t} \right) \quad (11)$$

2.4. Kerr Coefficient

To allow the optical control of the Casimir force, a laser beam is introduced to induce the AC Kerr effect, and the electric permittivity ε is

$$\varepsilon = \varepsilon_0 + \chi_{ij}^{(3)} |E|^2 \quad (12)$$

where ij is the index of the change in ε tensor, and $\chi_{ij}^{(3)} = \chi^{(3)} \cdot \delta_{ij}$. Thus, we use the Kerr material instead of laser field to simulate the Casimir force in above geometry. Below, we introduce a coefficient K that $K = \chi^{(3)}$.

Finally, the expression for the Casimir force becomes

$$F_i = \int_0^\infty dt \text{Im}[g(-t)] \times \sum_n \int_S ds_j(r, z) f_n(r, z) \Gamma_{ij;n}(r, z, t) \quad (13)$$

with

$$\Gamma_{ij;n}(r, z, t) = 2 \sum_{m>0} \text{Re}[\Gamma_{ij;n,m}(r, z, t)] \quad (14)$$

3. RESULTS AND ANALYSES

3.1. Ideal Metal Material

Before we consider the anisotropic materials, the ideal metal material was used in the simulations. An ideal metal ellipsoid was set above an ideal metal plate with a circular hole in vacuum. Here, the size of ellipsoid as sketched in Fig. 1 with $r_r = 50$ nm, $r_z = 250$ nm, thickness of plate $t = 100$ nm, diameter of circular hole on the plate $w = 2$ μm , and electric permittivity $\varepsilon_0 = 1$. Repulsion was undoubtedly occurred as the green line shown in Fig. 2. Then we introduce the Kerr effect ($K = 0.01$) by placing a laser on the ellipsoid or the plate or the medium surrounded them. When a laser beam was placed on the ellipsoid, as the black line shown in Fig. 2, the repulsion is weak and approximate to 0; the red dashed line shows that a laser beam was placed on the plate; the blue dotted line shows that when a laser beam was placed in vacuum, the curve became fluctuated, and compared with the green line, it clearly shows the nonlinear effect.

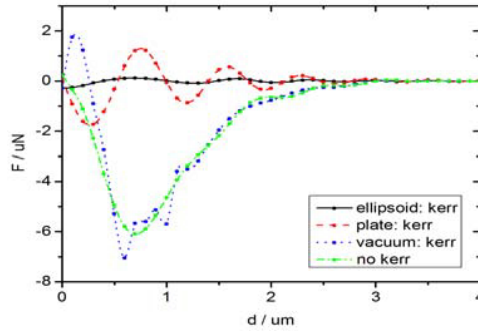


Figure 2. Casimir interaction and Kerr effect with a laser beam at different location: the green line shows results without laser beam; the black line indicates a laser beam was placed on the ellipsoid; the red line indicates a laser beam was placed on the plate; the blue line indicates a laser beam was placed in vacuum.

We fixed the ellipsoid and placed a laser on it. In Fig. 3, we plot the dependence of the Casimir force on laser intensity for different separation d between metallic ellipsoid and plate.

3.2. Anisotropic Material in Vacuum

Now we begin to consider the anisotropic material and set the ellipsoid $\varepsilon_1 = \text{diag}(1 \ 1 \ 12)$ from Eq. (1). With an anisotropic ellipsoid and an ideal metal plate as shown in Fig. 4, it is noted that the amplitude of the force is extremely different between the black linear line and the red nonlinear line. The curve in black is flat ranging from 0 to 1.5 μm where the curve in red is fluctuated. The peak value of the red line arrives at 0.6 μN and the bottom value at -1.5 μN ; with an anisotropic ellipsoid and an anisotropic plate as shown in Fig. 5, the amplitude of the red nonlinear line is less than the black linear line. The

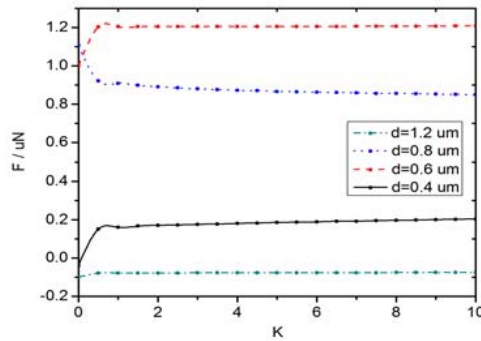


Figure 3. Casimir force between ideal metal ellipsoid and ideal metal plate with different d , as a function of intensity of incident laser K . The red and black lines show that when $d = 0.6 \mu\text{m}$ and $d = 0.4 \mu\text{m}$, the force is increased with the rise of K ; the blue line shows that when $d = 0.8 \mu\text{m}$, the force is decreased with the rise of K ; the cyan line shows that when $d = 1.2 \mu\text{m}$, the force is almost not changed.

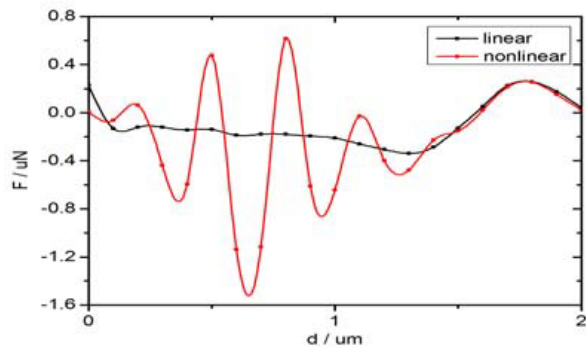


Figure 4. Casimir force between an anisotropic ellipsoid and ideal metal plate in vacuum. The black line shows the ellipsoid without a laser, in contrast, the red line shows a laser was placed on the ellipsoid $K = 0.01$.

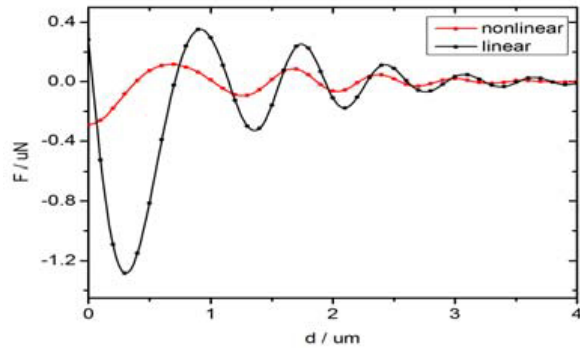


Figure 5. Casimir force between an anisotropic ellipsoid and anisotropic plate. Both the electric permittivity $\epsilon_0 = \epsilon_1$. The red line shows that a laser was placed on the ellipsoid, in contrast, the black line shows without. $K = 0.01$.

Kerr effect enhances the force when the plate is ideal metal (Fig. 4), but reduces the force when the plate is anisotropic material (Fig. 5). However, the Casimir force between anisotropic materials is much weaker than metallic materials.

In order to view the dependence of the Casimir force on laser intensity for different separation d and minor diameter of the ellipsoid r_r clearly, we re-plot the results with 3D graphs (See Fig. 6). Fig. 6(a) shows no laser on the anisotropic ellipsoid, as a basic contrast to (b) and (c). The maximum value of the force indicates the attractive force $F_a \approx 3 \mu\text{N}$, and the minimum value of the force indicates the repulsive force $F_r \approx 1.5 \mu\text{N}$. Fig. 6(b) shows when a laser based on the anisotropic ellipsoid with intensity $K = 0.01$, the force becomes stronger but not flat because of the nonlinear effect. The attractive force $F_a \approx 5 \mu\text{N}$, and the repulsive force $F_r \approx 3 \mu\text{N}$. Fig. 6(c) shows that when the intensity of laser $K = 1$, the force becomes even stronger and more fluctuated. The attractive force $F_a \approx 10 \mu\text{N}$, and the repulsive force $F_r \approx 10 \mu\text{N}$. Therefore, the Kerr effect can tune and enhance the Casimir force between an anisotropic ellipsoid and an ideal metal plate in vacuum.

When both the ellipsoid's and plate's permittivities are $\epsilon_1 = \text{diag}(1 \ 1 \ 12)$, and both are placed a laser on them. From Fig. 7, we can see that the Casimir force is even weaker than the results in Fig. 6. Clearly, the anisotropic material with Kerr effect can reduce the Casimir force.

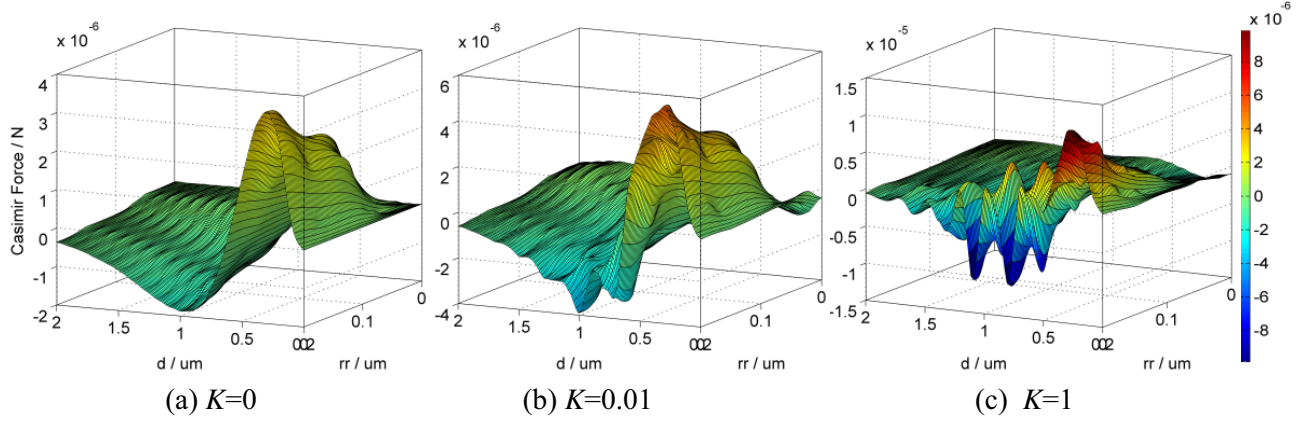


Figure 6. 3D plot of the Casimir force between an anisotropic ellipsoid and an ideal metal plate in vacuum, as a function of separation d and minor diameter of the ellipsoid r_r . The electric permittivity of ellipsoid is $\varepsilon_1 = \text{diag}(1 \ 1 \ 12)$. (a) $K = 0$ indicates no laser on the ellipsoid; (b) a laser was placed on the ellipsoid and $K = 0.01$; (c) $K = 1$.

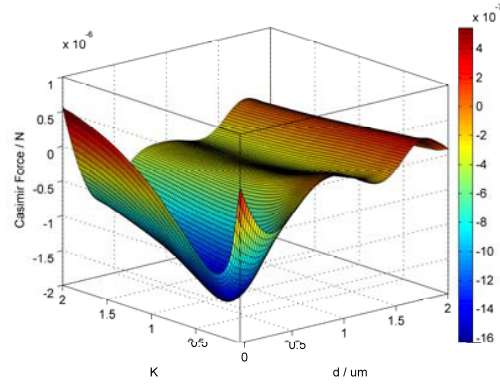


Figure 7. 3D plot of the Casimir force between an anisotropic ellipsoid and an anisotropic plate in vacuum, both the permittivity are $\varepsilon_1 = \text{diag}(1 \ 1 \ 12)$, as a function of separation d and intensity of laser K .

3.3. Anisotropic Material Embedded in Anisotropic Medium

As discussed above, we have placed the geometry model in vacuum, and how about embedded in other environments? Then we begin to consider replacing the vacuum by the other anisotropic material, and the electric permittivity is $\varepsilon_2 = \text{diag}(12 \ 12 \ 1)$. As shown in Fig. 8. The amplitude of the force in cyan is the strongest. The peak value arrives at $40 \mu\text{N}$, the bottom value at $100 \mu\text{N}$, and the amplitude of the force in black is the weakest. We can see its maximum value from the left inset, in which $F = 0.002 \mu\text{N}$ approximate to 0 (See the inset figures), and the bottom value in blue is a bit stronger than the value in red, approximate to 2.5 times. When $d > 0.2 \mu\text{m}$, all the repulsive forces are turned into attractive force, and when $d > 0.8 \mu\text{m}$, all the forces diminish to 0. Thus, the Kerr effect can reduce the Casimir force between anisotropic ellipsoid and anisotropic plate in anisotropic medium. However, the Casimir force between ideal metal ellipsoid and plate in anisotropic medium is enhanced by the Kerr effect.

Considering the case with the structure immersed in anisotropic medium, we found an interesting phenomenon. The results are shown in Fig. 9. When we placed only one laser on the ideal metal ellipsoid, as shown in (a) $K \in (0, 0.2)$ and (b) $K \in (0, 2)$, the force was almost repulsive, and the maximum of repulsive force $F_r \approx 1.4 \times 10^{-9} \text{N}$. When two lasers of the same intensity were placed on the ellipsoid and plate separately, as shown in (c) $K \in (0, 0.2)$ and (d) $K \in (0, 2)$, the force was attractive, and the maximum attractive force $F_a \approx 1.6 \times 10^{-9} \text{N}$. As we have proved above, the force between anisotropic materials is much smaller, and we can make use of them in control more feasible force in NEMS.

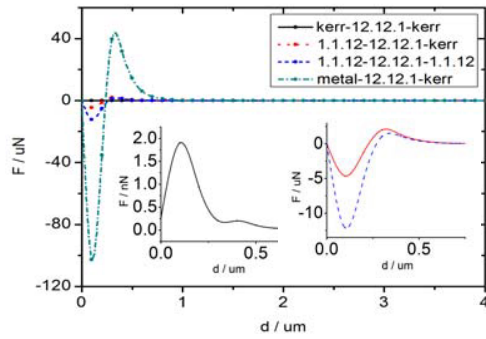


Figure 8. Casimir force between different materials' ellipsoid and plate: the black line shows that the two same intensity of lasers were placed on the ideal metal ellipsoid and plate separately, the medium vacuum was replaced by anisotropic material ϵ_2 ; the red line shows that a laser was placed on the ideal metal plate, the electric permittivity of ellipsoid is ϵ_1 , the electric permittivity of medium is ϵ_2 ; the blue line shows that both the electric permittivity of ellipsoid and plate are ϵ_1 , the electric permittivity of medium is ϵ_2 ; the cyan line shows that only a laser was placed on the ideal metal plate, the electric permittivity of medium is ϵ_2 . The insets are the corresponding zoom in results with $K = 0.01$.

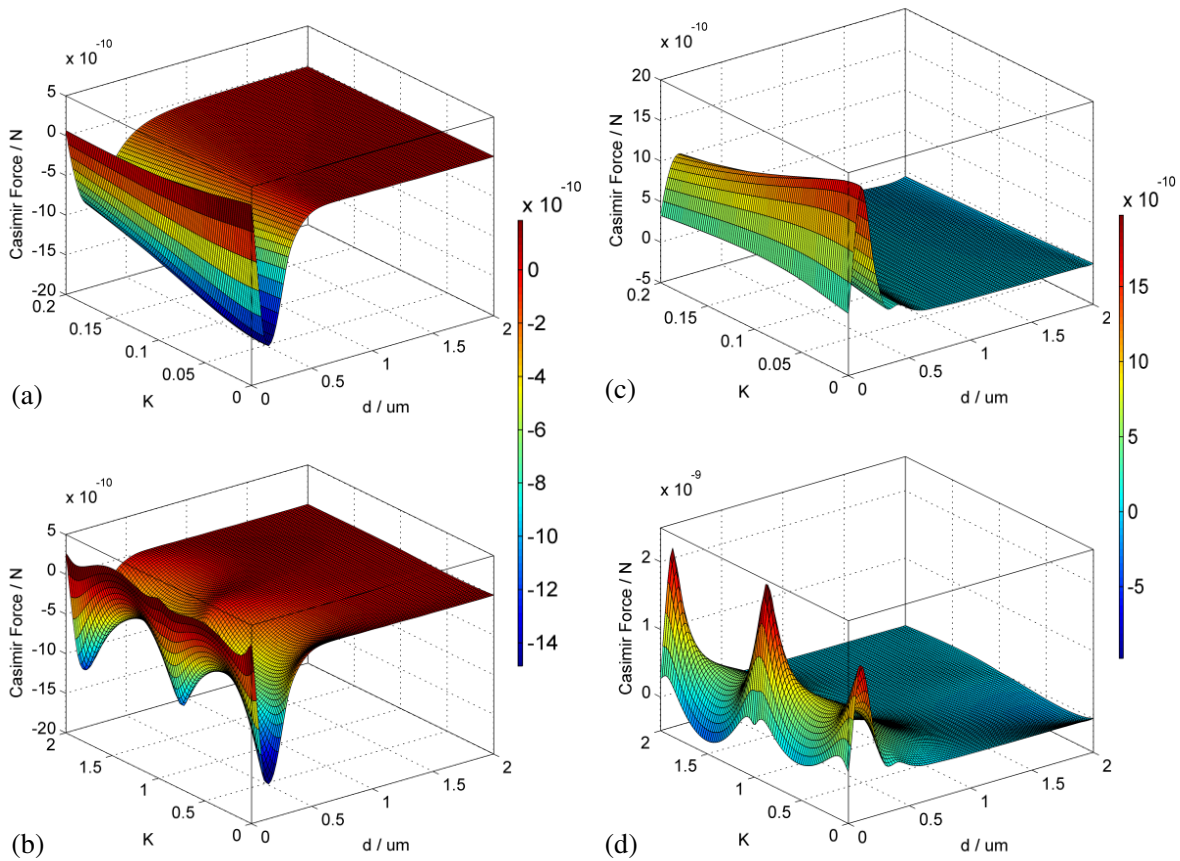


Figure 9. 3D plot of the Casimir force between an ideal metal ellipsoid and an ideal metal plate in anisotropic material ϵ_2 , as a function of separation d and the intensity of laser K . (a) $K \in (0, 0.2)$ and (b) $K \in (0, 2)$: a laser was placed on the ellipsoid; (c) $K \in (0, 0.2)$ and (d) $K \in (0, 2)$.

4. CONCLUSIONS

Based on the Maxwell's stress tensor, we analyze the Casimir force using combinations of anisotropic materials and nonlinear material exhibiting AC Kerr effect. We show that the force can be significantly varied by changing the intensity and location of the laser, as well as the properties of the anisotropic materials. The sensitive changing provides new convenience to solve some practical problems in NEMS, such as manipulate nano-resonators and integrate optical devices into NEMS.

ACKNOWLEDGMENT

This work is supported in part by the National Natural Science Foundation of China (Nos. 51277001, 61101064, 61471001), in part by the NCET (No. NCET-12-0596), and in part by the DFMEC (No. 20123401110009).

REFERENCES

1. Casimir, H. B. G., "On the attraction between two perfectly conducting plates," *Proc. K. Ned. Akad. Wet.*, Vol. 51, 793–795, 1948.
2. Atkins, P. R., Q. I. Dai, W. E. I. Sha, and W. C. Chew, "Casimir force for arbitrary objects using the argument principle and boundary element methods," *Progress In Electromagnetics Research*, Vol. 142, 615–624, 2013.
3. Bordag, M., U. Mohideen, and V. M. Mostepaneko, "New developments in the Casimir effect," *Phys. Rep.*, Vol. 353, 1, 2001.
4. Klimchitskaya, G. L., U. Mohideen, and V. M. Mostepanenko, "Casimir and van der Waals forces between two plates or a sphere (lens) above a plate made of real metals," *Phys. Rev. A*, Vol. 61, 062107, 2000.
5. Rodriguez, A., M. Ibanescu, D. Iannuzzi, F. Capasso, J. D. Joannopoulos, and S. G. Johnson, "Computation and visualization of casimir forces in arbitrary geometries: Nonmonotonic lateral-wall forces and the failure of proximity-force approximations," *Phys. Rev. Lett.*, Vol. 99, 080401, 2007.
6. Rahi, S. J., M. Kardar, and T. Emig, "Constraints on stable equilibria with fluctuation-induced (Casimir) forces," *Phys. Rev. Lett.*, Vol. 105, 070404, 2010.
7. Lambrecht, A. and V. N. Marachevsky, "Casimir interaction of dielectric gratings," *Phys. Rev. Lett.*, Vol. 101, 160403, 2008.
8. Yang, Y., R. Zeng, H. Chen, S. Zhu, and M. S. Zubairy, "Controlling the Casimir force via the electromagnetic properties of materials," *Phys. Rev. A*, Vol. 81, 022114, 2010.
9. Serry, F. M., D. Walliser, and G. J. Maclay, "The role of the Casimir effect in the static deflection and stiction of membrane strips in microelectromechanical systems (MEMS)," *J. Appl. Phys.*, Vol. 84, 2501, 1998.
10. De Los Santos, H. J., "Nanoelectromechanical quantum circuits and systems," *Proc. IEEE*, Vol. 91, 1907, 2003.
11. Chan, H. B., V. A. Aksyuk, R. N. Kleiman, D. J. Bishop, and F. Capasso, "Nonlinear micromechanical casimir oscillator," *Phys. Rev. Lett.*, Vol. 87, 211801, 2001.
12. Capasso, F., J. N. Munday, D. Iannuzzi, and H. B. Chan, "Casimir forces and quantum electrodynamic torques: Physics and nanomechanics," *IEEE. J. Quantum. Electron.*, Vol. 13, 400, 2007.
13. Levin, M., A. P. McCauley, A. W. Rodriguez, M. T. H. Reid, and S. G. Johnson, "Casimir repulsion between metallic objects in vacuum," *Phys. Rev. Lett.*, Vol. 105, 090403, 2010.
14. Munday, J. N., F. Capasso, and V. A. Parsegian, "Measured long-range repulsive Casimir-Lifshitz forces," *Nature*, Vol. 457, 170–173, 2009.
15. Chen, R. P. and C. H. R. Ooi, "Evolution and collapse of a Lorentz beam in kerr medium," *Progress In Electromagnetics Research*, Vol. 121, 39–52, 2011.

16. Ooi, C. H. R. and Y. Y. Khoo, "Controlling the repulsive Casimir force with the optical Kerr effect," *Phys. Rev. A*, Vol. 86, 062509, 2012.
17. Huang, Z. X., T. Koschny, and C. M. Soukoulis, "Theory of pump-probe experiments of metallic metamaterials coupled to the gain medium," *Phys. Rev. Lett.*, Vol. 108, 187402, 2012.
18. Rodriguez, A. W., M. Ibanescu, D. Iannuzzi, J. D. Joannopoulos, and S. G. Johnson, "Virtual photons in imaginary time: Computing exact Casimir forces via standard numerical-electromagnetism techniques," *Phys. Rev. A*, Vol. 76, 032106, 2007.
19. Rodriguez, A. W., A. P. McCauley, J. D. Joannopoulos, and S. G. Johnson, "Casimir forces in the time domain: Theory," *Phys. Rev. A*, Vol. 80, 012115, 2009.
20. Brown, L. S. and G. J. Maclay, "Vacuum stress between conducting plates: An image solution," *Phys. Rev. A*, Vol. 184, 1272, 1969.